



Article

Variations in the Growth of Cotyledons and Initial True Leaves as Affected by Photosynthetic Photon Flux Density at Individual Seedlings and Nutrients

Eri Hayashi ^{1,2,*}, Yumiko Amagai ^{1,3} , Toyoki Kozai ¹, Toru Maruo ¹, Satoru Tsukagoshi ³ , Akimasa Nakano ² and Masahumi Johkan ²

¹ Japan Plant Factory Association, 6-2-1 Kashiwanoha, Kashiwa 277-0882, Japan; amagai@npoplantfactory.org (Y.A.); kozai@faculty.chiba-u.jp (T.K.); maruo@faculty.chiba-u.jp (T.M.)

² Graduate School of Horticulture, Chiba University, 648 Matsudo, Matsudo 271-8510, Japan; anakano@chiba-u.jp (A.N.); johkan@faculty.chiba-u.jp (M.J.)

³ Center for Environment, Health and Field Sciences, Chiba University, 6-2-1 Kashiwanoha, Kashiwa 277-0882, Japan; tsukag@faculty.chiba-u.jp

* Correspondence: ehayashi@npoplantfactory.org; Tel.: +81-47-137-8318



Citation: Hayashi, E.; Amagai, Y.; Kozai, T.; Maruo, T.; Tsukagoshi, S.; Nakano, A.; Johkan, M. Variations in the Growth of Cotyledons and Initial True Leaves as Affected by Photosynthetic Photon Flux Density at Individual Seedlings and Nutrients. *Agronomy* **2022**, *12*, 194. <https://doi.org/10.3390/agronomy12010194>

Academic Editor: Monica Boscaiu

Received: 30 December 2021

Accepted: 10 January 2022

Published: 13 January 2022

Publisher's Note: MDPI stays neutral with regard to jurisdictional claims in published maps and institutional affiliations.



Copyright: © 2022 by the authors. Licensee MDPI, Basel, Switzerland. This article is an open access article distributed under the terms and conditions of the Creative Commons Attribution (CC BY) license (<https://creativecommons.org/licenses/by/4.0/>).

Abstract: Plant factories with artificial lighting (PFALs), with well-insulated and airtight structures, enable the production of large quantities of high-quality plants year-round while achieving high resource use efficiency. However, despite the controlled environment in PFALs, variations in plant individuals have been found, which affect productivity in PFAL operations. Plant phenotyping plays a crucial role in understanding how the surrounding microenvironment affects variations in plant phenotypes. In the current study, a modular phenotyping system for seedling production was developed, focusing on practicality and scalability in commercial PFALs. Experiments on seedlings, which strongly affect productivity, were conducted to obtain cotyledon unfolding time and the time series projected area of cotyledons and true leaves of individual seedlings of romaine lettuce (*Lactuca sativa* L. var. longifolia), using RGB images. This was also undertaken to analyze how the surrounding microenvironment of photosynthetic photon flux densities and nutrients affect growth variations for plant cohort research. In agreement with the actual measurements, variations in seedling growth were identified even under similar microenvironments. Furthermore, the results demonstrated larger variations in seedlings with higher relative growth. Aiming for simplified interactions of phenotypes with the microenvironment, management, and genotype, seedling selection and breeding with plant production in PFALs may enable plant uniformity and higher productivity.

Keywords: time series projected leaf area; cotyledon unfolding time; horizontal PPFD; microenvironment; growth rate; phenotyping; plant cohort research; plant factory with artificial lighting (PFAL); productivity

1. Introduction

Plant factories with artificial lighting (PFALs), with an almost airtight and well-insulated structure, have the potential to enable the production of large quantities of high-quality plants year-round while achieving high efficiency of resource utilization [1–10]. The theoretical benefits of PFAL can be achieved only when the system is properly engineered, constructed, and operated [11–13]. In actuality, a variety of PFAL challenges remain, including high initial investment, optimal cultivation system, and environmental controls, which can be solved by improving productivity in PFALs [13].

Despite the controlled environment in PFALs, variations in plant individuals have been found, particularly around harvesting, which results in a negative effect on plant productivity in PFAL operations [5,14,15]. The uniformity of plant growth by reducing two-dimensional (2D) variations in plant traits (i.e., phenotype), such as fresh weight, plant height, morphology, and concentrations of secondary metabolites per plant, can

contribute to productivity improvement in PFALs [14]. Variations in the plant traits of individual plants are mainly ascribed to three factors: environment, genotype (species and cultivar), and management (human and machine intervention) [5,14]. Indeed, 2D variations in plant traits over a cultivation tray are partly attributed to 2D variations in the surrounding microenvironment of individual plants, including photosynthetic photon flux density (PPFD) and air current speed over and within the plant canopy or individuals in the tray [14]. Past studies have shed light on the PPFD distribution in the cultivation tray, and even the difference in the PPFD distribution between a plant canopy and the cultivation tray without plants [16–18].

Plant phenotyping plays an integral role in understanding how the microenvironment surrounding individual plants affects variations in the phenotype of individual plants [5,14,19]. Plant phenotyping is a set of methodologies and protocols used to study plant performance, growth, architecture, and composition at different scales of organization, from organs to canopies, and it elucidates the plant trait dynamics in a non-destructive and non-invasive manner [5,14,19–21]. Having great potential for application to commercial PFALs [22], image-based studies in PFALs have been conducted, including quantifying the projected leaf area (value measured by 2D camera images captured from above the plant canopy or seedling trays) of the plant canopy [15,23–28].

Cotyledons are the first leaves that appear on a plant and play a crucial role in the development of seedlings, particularly in the early stages, which affects the subsequent plant growth process [29–32]. During the initial growth stage of leaf development, leaf tissues are built and require carbon and energy from other parts of the plant [33,34]. At the seedling stage, plants are dependent on the immediate establishment of photosynthesis, leading to shoot development, which mainly depends on the photosynthetic capacity of the cotyledon and stored nitrogen [34]. Early photosynthesis by the cotyledon is essential for seedling growth [32]. Therefore, to achieve maximal plant growth, PPFD and nutrient availability are environmental factors that strongly affect plant growth from the early developmental stages of seedlings onwards [34,35].

However, most previous studies on the cotyledon and initial stage of seedlings have been limited to the mean values of plant population, not the individual plants, alongside average PPFD, not the PPFD at individual plants. Furthermore, most image-based analyses or quantification of the projected leaf area of seedlings in PFALs have been conducted only after the emergence of true leaves. The frequency of image capture has been confined to a few times per day or even per week. Therefore, to elucidate the variations in the growth of cotyledons and initial true leaves, and how this is affected by the PPFD and nutrients, which are the essential factors for the initial development of plants, it is crucial to measure cotyledon unfolding time and the time series projected leaf area together with ground truth measurements, and analyze how the microenvironment of PPFD at individual seedlings and nutrients affects individual growth.

A modular plant phenotype measurement system for seedling production was developed, focusing on practicality and scalability in commercial PFALs, and achieved low cost using small cameras and sensors, and a cultivation method similar to that of commercial PFALs. In this study, the initial stage of seedlings, one of the critical early stages of plant growth, was used as part of research that examined the entire plant life cycle. Experiments were conducted to obtain cotyledon unfolding time and the time series projected leaf area of cotyledons and true leaves of individual seedlings of romaine lettuce (*Lactuca sativa* L. var. longifolia), using 2D camera images. This was also undertaken to analyze how the surrounding microenvironment of PPFD and nutrients affects the variations in the growth of individual seedlings for plant cohort research. Considering leaf movement [15,36,37], red-green-blue (RGB) images were acquired and processed every 0.5 h.

In plant cohort research, the life cycle phenome history of individual plants can be captured continuously and noninvasively, and analyzed from seed sowing to harvesting using phenotyping units, together with the time series data on environment, managerial, and resource inputs and outputs in PFALs [4–6,14,38]. Using the time series datasets

in the data warehouse, plant cohort research makes it possible to identify optimal set points of environmental factors for maximizing multi-objective functions and concurrently improving plant productivity, selection of seedlings for grading, and breeding new cultivars in PFALs [4–6,14,38].

Through this study, cotyledon unfolding time and the time series projected area of cotyledons and true leaves of individual seedlings were obtained, using time series RGB images. In agreement with the actual individual measurements, variations in seedling growth were identified, even under similar microenvironments. Furthermore, the results demonstrated larger variations in seedlings with higher relative growth.

2. Materials and Methods

2.1. Description of the System

A modular seedling production system (MSPS) was developed by improving the germination container box (GCB) equipped with a phenotyping unit and air temperature and relative humidity sensors [5] as a serial study for plant cohort research in PFALs. Figure 1 shows a configuration diagram of the MSPS composed of eight units and parts. The additionally installed items in the GCB included LEDs, an air circulator, and a digital weight scale with data loggers (L, M, and N, respectively; Figure 1a–c).

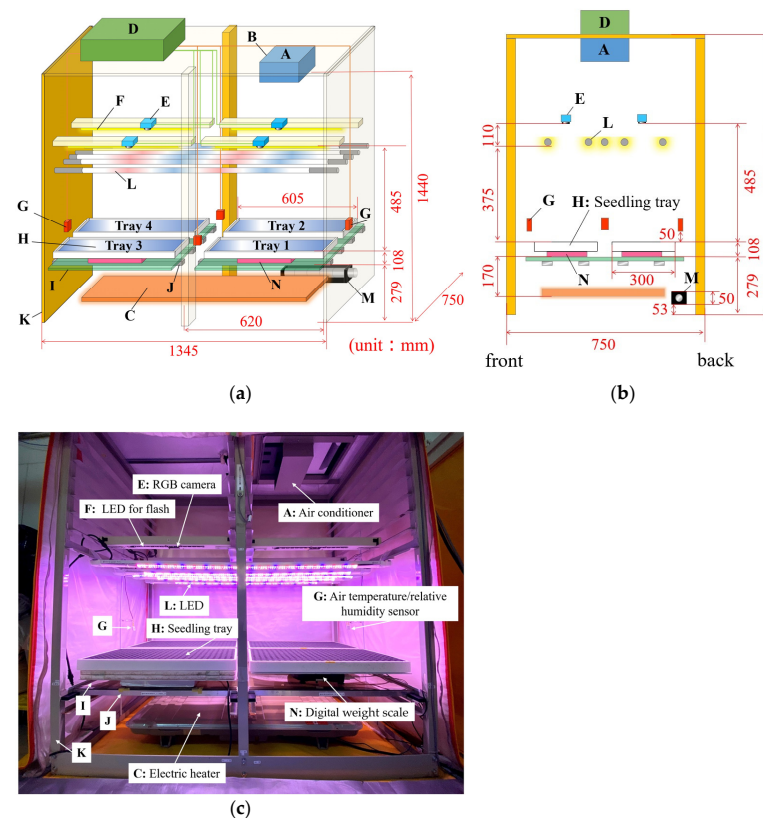


Figure 1. Modular seedling production system (MSPS) equipped with phenotyping unit and air temperature and relative humidity sensors. (a) Schematic diagram. (1) Temperature control unit: air conditioner (A), air outlet of the air conditioner (B), electric heater (C). (2) Phenotyping unit: control board ($\times 4$) (D), red-green-blue (RGB) camera ($\times 4$) (E), white light-emitting diode (LED) for flash ($\times 4$) (F). (3) Air temperature and relative humidity sensor ($\times 4$) (G). (4) Cultivation unit: seedling tray with the substrate (seedling tray) ($\times 4$) (H), acrylic plate (I), reinforcement bar (J). (5) Exterior box with frame (K). [5] (6) LED (18 W each, length 1170 \times width 30 \times height 25 mm) (ZK-TB18-VE02/A; Fujian Sanan Sino-Science Photobiotech Co., Ltd., Fujian, China) ($\times 5$) (L). (7) Air circulator (DC12V 0.2A, blade size: 30 \times 190 mm, length 240 \times width 48 \times height 50 mm) (a15110600ux0249jp; Uxcell, Hong Kong, China) (M), and (8) digital weight scale (linearity error ± 300 mg, precision 100 mg) ($\times 3$) with data loggers ($\times 2$) (N). (b) Schematic diagram from the side. (c) Inside view of MSPS.

The phenotyping units, sets of RGB cameras (Raspberry Pi Pi NoIR Camera Module V2; Raspberry Pi Foundation, Cambridge, UK) ($\times 4$), and white LEDs for the flash of the RGB cameras (15 white LED tape, length 300 mm; SOF-15W-30-3SMD; Tokulumi Co., Ltd., Kwai Chung, Hong Kong, China) ($\times 4$) [5] were set 485 mm above the surface of each seedling tray (E and F, respectively; Figure 1a–c). Additionally, four air temperature and relative humidity (*Tin* and *RH* respectively) sensors were placed 50 mm above the right or left of the surface of the seedling trays. The phenotyping unit, consisting of RGB cameras and white LEDs for the flash, and *Tin* and *RH* sensors were connected to each control board (Raspberry Pi 3 Model B; Raspberry Pi Foundation, Cambridge, UK) ($\times 4$), and activated every ten minutes [5]. These data were automatically sent to a data warehouse (DWH) through control boards [5,39].

Seedling trays were placed consistently at each designated location. For this study, two trays on the right side (Trays 1 and 2) of four in the MSPS were used, and the remaining two trays on the left (Trays 3 and 4) were also filled with the same plants simultaneously for another analysis (Figure 1a–c).

2.2. Light Environment for Individual Seedlings

To study the growth variations in the seedlings as affected by the PPF, a light environment was designed to maximize the distribution of horizontal PPF over the seedling tray in conjunction with minimizing the PPF variations between the two seedling trays (Tray 1 with the water and Tray 2 with the nutrient solution (nutrients)) (Figure 1a, Table 1). Therefore, to set the desired PPF distribution over the tray, both side edges of five LEDs, except the one in the middle, were covered with aluminum tape.

Table 1. Treatments and codes of the experiment. The distributions of horizontal PPF within the trays (width 605 \times length 300 mm) were set for this study. Here, 18 different PPFs in each tray (Tray 1 with the water and Tray 2 with the nutrients) were categorized into three classifications (6 PPFs/classification) based on the level of PPF: low (L), medium (M), and high (H), $84 \leq 126$, $126 < 166$, $166 \leq 208 \mu\text{mol m}^{-2} \text{s}^{-1}$, respectively.

Code	Nutrients/Water	PPF Classifications	Distribution of Horizontal PPF ($\mu\text{mol m}^{-2} \text{s}^{-1}$)
Nutrients-H	Nutrients (Tray 2)	High	175, 181, 187, 195, 202, 208
Nutrients-M		Medium	140, 145, 147, 148, 151, 165
Nutrients-L		Low	84, 102, 102, 104, 118, 126
Water-H	Water (Tray 1)	High	168, 175, 181, 190, 197, 205
Water-M		Medium	136, 142, 144, 148, 153, 161
Water-L		Low	84, 100, 104, 112, 121, 123

First, each seedling tray (605 \times 300 \times 42 mm), having a black substrate inside 300 plants (tray), was divided into 18 sections. Then, horizontal PPF 0.04 m above the surface of the tray was measured at each section using PPF sensors (accuracy $\pm 5\%$) (LI-190R; LI-COR, Inc., Lincoln, NE, USA) with a data logger. The distributions of horizontal PPF within the trays are shown in Table 1: from the minimum 84 to the maximum 205 (Tray 1) or 208 (Tray 2) $\mu\text{mol m}^{-2} \text{s}^{-1}$. The 18 different PPFs in each tray were categorized into three classifications (6 PPFs/classification) based on the level of PPF: low (L), medium (M), and high (H), as $84 \leq 126$, $126 < 166$, and $166 \leq 208 \mu\text{mol m}^{-2} \text{s}^{-1}$, respectively (Table 1).

For the experiments, two representative plants from 16 or 20 plants in each section closest to the PPF sensor were chosen (2×18 PPFs/tray $\times 2 = 72$ representative plants). Therefore, there were 12 representative plants for each treatment (2×6 PPFs/treatment $\times 3$ PPF classifications $\times 2$ (nutrients/water) = 72 representative plants) (Table 1). If the representative plants did not germinate, the plants next to the original representative plants were selected. The remaining seedlings, other than 72 representative plants, were also cultivated together, as there were 300 plants in each tray, following a cultivation method

similar to that used for commercial PFALs. The average ratio of the LED spectrum, blue: green: red: farRed, at the trays, was 13:16:60:11.

2.3. Hours to Cotyledon Unfolding and Projected Area of Cotyledon and True Leaves of Individual Plants Estimated with Time Series RGB Images

In this study, an RGB camera was used to obtain 2D image data every 0.5 h to estimate the hours required for cotyledon unfolding (H_c : the time from sowing to the unfolding of the cotyledon of individual plants) and the time course of the projected area of the cotyledon ($Ap-c$), true leaf ($Ap-t$), and cotyledon and true leaf ($Ap-ct$) of individual seedlings at intervals of 0.5 h (See Table 2 for abbreviations). In the case of a failure of image capturing, the RGB image acquired ten minutes before the scheduled timing was used because the raw image data were automatically captured every ten minutes.

Table 2. List of symbols, variable names with descriptions and units.

Symbol	Variable Name/Description	Unit
Ac, \overline{Ac}	Cotyledon area of individual plant 216 h after sowing (HAS), and their average	mm ²
Act, \overline{Act}	Area of cotyledon and true leaves of individual plant 216 HAS, and their average	mm ²
At, \overline{At}	True leaf area of individual plant 216 HAS, and their average	mm ²
$Ap-c, \overline{Ap-c}$	Projected cotyledon area of individual plant, and their average	mm ²
$Ap-ct, \overline{Ap-ct}$	Projected area of cotyledon and true leaves of individual plant, and their average	mm ²
$Ap-t, \overline{Ap-t}$	Projected true leaf area of individual plant, and their average	mm ²
Hc, \overline{Hc}	Hours to cotyledon unfolding (from sowing to the unfolding of the cotyledon) of individual plant, and their average	h
LAR	The ratio of leaf area (Act) to shoot dry weight (Wd) (Act divided by Wd)	m ² g ⁻¹
Lh, \overline{Lh}	Hypocotyl length of individual plant 216 HAS, and their average	mm
Integrated PPFD	Integrated PPFD during hours from cotyledon unfolding (Hc) to 216 HAS of individual plant	mol m ⁻²
PPFD	Horizontal photosynthetic photon flux density at individual plant 0.04 m above the surface of the tray	μmol m ⁻² s ⁻¹
VPNS	Volumetric percentage of nutrient solution in the tray [5]	%
Wd, \overline{Wd}	Shoot (ct, h , and petiole) dry weight of individual plant 216 HAS, and their average	mg/plant
Wf, \overline{Wf}	Shoot fresh weight of individual plant 216 HAS, and their average	mg/plant

Each RGB image, which covered one tray with 300 seedlings, was first divided into 18–300 images depending on the size of the seedlings for ease of image processing. Then, the time series RGB images of each seedling were re-sequenced in chronological order with 0.5 h intervals [5] (Figure 2a).

To estimate H_c , the first RGB image with a clearly visible unfolded cotyledon, which achieved the most horizontal position, was selected among the time-course images of individual seedlings in chronological order [5]. Then, to estimate the projected areas of cotyledons and true leaves, each RGB image of individual seedlings, in chronological order, was imported into graphic editor software (Photoshop, Adobe Inc., San Jose, CA, USA) to carefully eliminate the background from the image so that only time series images of cotyledons and true leaves remained (Figure 2b). The backgrounds of individual cotyledons and true leaves were carefully eliminated with zoomed images, particularly in the case of overlapping leaves and the attached seed coats, as coated seeds were used in this study (Figure 2a,b). Furthermore, time series images of cotyledons and true leaves were divided into different images so that $Ap-c$ and $Ap-t$ could be estimated separately (Figure 2a,b).

To estimate $Ap-c$ and $Ap-t$, ImageJ, a Java-based open software package for image processing, was used [40]. Before importing the edited images, the scale was set by associating the distance in pixels with the actual distance between each substrate hole in the raw images. The scale was selected based on the number of pixels per millimeter. The edited time series images were processed into binary images, and the threshold was set to acquire the projected areas. Separated time series $Ap-c$ and $Ap-t$ of the individual seedlings were estimated, along with $Ap-ct$, the sum of individual $Ap-c$ and $Ap-t$. To identify the

accuracy of horizontal projected leaf areas that were possibly affected by the camera angle of view, 52 same-sized square pieces of paper, as a substitute for the plants, were placed horizontally in the tray in an equidistant manner, and the RGB images were captured. The accuracy of the 52 area values using ImageJ among the tray was $\pm 5\%$. In this study, the projected images obtained from a single RGB camera covering one tray were used without adjusting the viewing angle or distortion correction, which possibly affected the estimation of some projected areas of the inclined leaves.

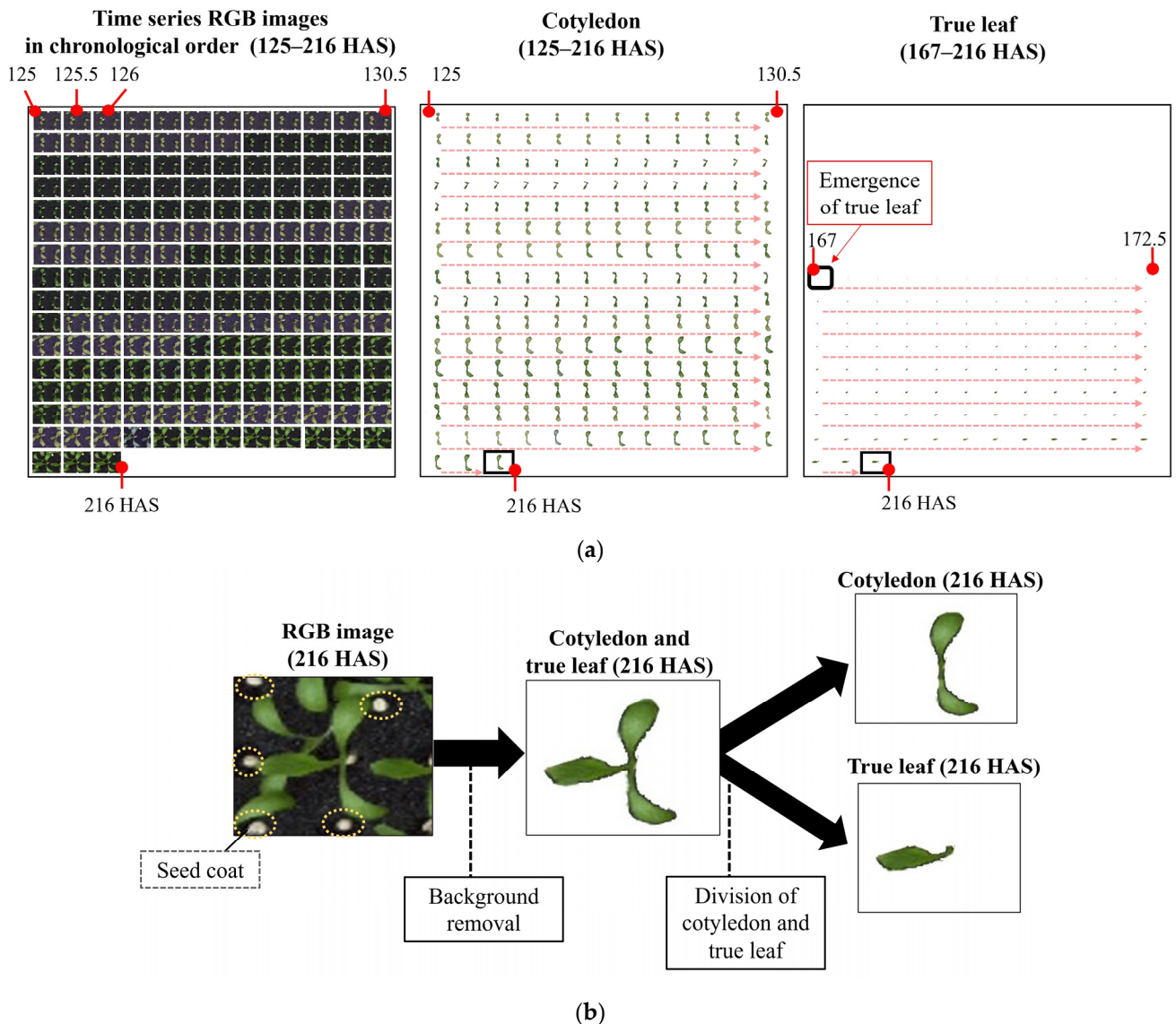


Figure 2. The time series RGB images of the same seedling, in chronological order, at 0.5 h intervals from 125 to 216 hours after sowing (HAS). This seedling, with nutrients and at high PPFD levels (Nutrients-H) ($202 \mu\text{mol m}^{-2} \text{s}^{-1}$), reached the largest projected area of cotyledon and true leaves among others 216 HAS. (a) Time series RGB images, time series images of cotyledon, and time series images of true leaf after its emergence. The cotyledon unfolding time was 66.5 h. (b) Magnified images of the same seedling at (a) 216 HAS: RGB image, cotyledon, and true leaf after background removal, and separated images of cotyledon and true leaf.

For the ground truth measurement, ImageJ was used to estimate areas of the cotyledons (A_c), true leaves (A_f), and cotyledons and true leaves (A_{ct}) of the individual seedlings 216 h after sowing (HAS) (See Table 2 for abbreviations). Separated cotyledons and true leaves of individual plants 216 HAS laid on the whiteboard together with a ruler were

photographed manually with a camera ($\alpha 6000$; SONY Corp., Tokyo, Japan) set at 0.675 m above the board, while maximizing the magnification of the lens.

The exact process for the projected areas was also carried out to estimate Ac , At , and Act , except for the scale setting process, in which the scale of a ruler was associated with the number of pixels per mm. Note that petioles of both cotyledons and true leaves of individual plants were not included in $Ap-c$, $Ap-t$, $Ap-ct$, Ac , At , and Act .

2.4. Experimental Design

2.4.1. Plant Material and Culture Conditions

To analyze the variations in the growth of cotyledons and initial true leaves as affected by PPFD at individual plants and the nutrients, experiments on seedlings were conducted from cotyledon unfolding to 216 HAS. Coated seeds of romaine lettuce (*Lactuca sativa* L. var. longifolia, Lomaria, TLE487, Takii & Co., Kyoto, Japan) were used. The average weight and percentage of dry matter of 100 uncoated seeds of the same variety were 1.4 mg and 92%, respectively. Black substrates made of flexible polyurethane foam (MIRAI Co., Ltd., Kashiwa, Japan, 584 × 280 × 28 mm, 300 wells, 12 mm in diameter × 6 mm deep) were used in the cultivation trays. Instead of the white substrate, a black substrate was chosen for this study to prevent light reflection from the surface of the substrate to the backside of the leaf surface.

The photoperiod was set to an average of 16 h per day. In addition to the light for cultivation, flashes for the RGB camera were set to 10 s/time for photographing every 10 min. Regarding the nutrient solution, Chiba University's lettuce formula [41] was used, with pH and electrical conductivity of 6.5 and 0.19 S m⁻¹, respectively. The volumetric percentage of the nutrient solution or water in the tray was 86% [5].

The air temperature inside the MSPS was set to 20 °C during the experimental period. Average T_{in} and RH ($\overline{T_{in}}$, \overline{RH}) during the photoperiod and dark period over 9 days were 21 ± 0.2 °C and 85 ± 2%, and 21 ± 0.6 °C, and 92 ± 2%, respectively. CO₂ concentrations during the photoperiod inside the MSPS were maintained at 1500 ± 50 μmol mol⁻¹. Air current speed 0.05 m above the surface of the trays was 0.16 ± 0.11 m s⁻¹, measured with a hot-wire anemometer (accuracy ± 2% or 0.02 m s⁻¹) (6531-21; KANOMAX JAPAN Inc., Suita, Osaka, Japan).

The MSPS was placed inside an environmentally controlled cultivation room under the hygienic conditions of PFAL at the Kashiwanoha Campus of Chiba University. The air temperature, relative humidity, and CO₂ concentrations inside the cultivation room were 20 °C, 80–100%, and 1470 ± 20 μmol mol⁻¹, respectively.

2.4.2. Data Acquisition, Variables, and Symbols

During the 9 days of cultivation, each RGB camera obtained 432 images (216 h × 0.5 h) per tray to estimate Hc and the time course of $Ap-c$, $Ap-t$, and $Ap-ct$. The time series projected areas of cotyledons and true leaves every 0.5 h of 72 seedlings (2 representative plants/the same PPFD × 18 different PPFDs × 2 trays either with the nutrients or the water) were estimated from cotyledon unfolding to 216 HAS. In total, approximately 300 (150 h × 0.5 h) time series projected areas per seedling were estimated, about 600 for both cotyledons and true leaves per seedling; thus, 43,200 projected areas for 72 seedlings.

In addition to the time course of the projected areas, actual manual measurements of 72 seedlings were individually conducted 216 HAS. As described in Table 2, in addition to Ac , At , and Act , shoot (cotyledon, true leaves, hypocotyl, and petiole) fresh weight, shoot dry weight (W_f and W_d , respectively), and hypocotyl length (L_h) were measured for each seedling 216 HAS. W_d was quantified after drying for two days at 80 °C in a thermostatic oven (accuracy ± 1 °C) (WFO-520W; TOKYO RIKAKIKAI Co., Ltd., Bunkyo-Ku, Tokyo, Japan). For weight measurement, a digital scale was used after calibration (linearity error ± 0.2 mg, precision 0.1 mg). A vernier caliper (instrumental error ± 0.03 mm) was used to measure L_h .

Additionally, the ratio of *Act* to *Wd* (*Act* divided by *Wd*) was calculated. To assess growth variations, the growth of each seedling was quantified and analyzed to determine how it was affected by the microenvironment of 18 different PPFs, during both the photoperiod and dark period, and the nutrients or water. Horizontal integrated PPF during hours from cotyledon unfolding (*Hc*) to 216 HAS of the individual plants (integrated PPF) was also calculated for the analysis.

3. Results

In this study, image data having an interval of 0.5 h were used to estimate *Hc* and projected areas of *Ap-c*, *Ap-t*, and *Ap-ct*. Figure 2 shows time series images of the same seedling in chronological order from 125 to 216 HAS as a case example among 72 seedlings. The seedling in Figure 2, with Nutrients-H (202 $\mu\text{mol m}^{-2} \text{s}^{-1}$), achieved the largest *Ap-ct* among 72 seedlings 216 HAS. Figure 2 shows time series RGB images in chronological order, time series images of cotyledon, and time series images of true leaf after its emergence. Additionally, magnified images of the same seedling 216 HAS: RGB image, cotyledon, and true leaf after removing background, and separated images of cotyledon and true leaf are shown in Figure 2b.

To analyze the variations in the growth of cotyledons and initial true leaves as affected by horizontal PPF at individual seedlings and nutrients and water, experiments on the initial stage of seedlings were conducted from cotyledon unfolding to 216 HAS. For the microenvironmental data, horizontal PPF 0.04 m above the surface of the tray at individual seedlings was measured (Table 1). Two seedling trays, together with either nutrients or water, were used, each with 18 different PPFs ranging from 84 to 205 or 208 $\mu\text{mol m}^{-2} \text{s}^{-1}$ (Table 1). In addition to the time course of the projected areas, actual manual measurements of 72 seedlings were individually conducted 216 HAS.

Figure 3 shows *Hc* and *Wd* of individual seedlings with nutrients and water. In this study, no specific effect of *Hc* on *Wd* was found, as illustrated in Figure 3. Most of the individuals resulted in an *Hc* of 63–70 h, except three seedlings with water that had *Hc* values of 77.5, 78.5, and 79 h, which led to the maximum 16 h difference between the largest and the smallest *Hc* (Figure 3). It appeared that even the majority of *Hc* (63–70 h) varied by a maximum of 7 h, although this occurred during the dark period in this study. The average *Hc* (\overline{Hc}) was 66.2 h with nutrients and 68 h with water; \overline{Hc} with nutrients was 1.8 h shorter than that with water.

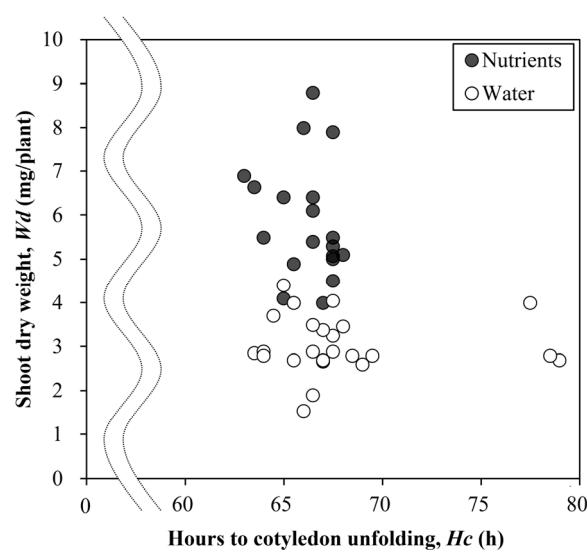


Figure 3. Hours to cotyledon unfolding (from sowing to the unfolding of the cotyledon) of individual plants (*Hc*) and shoot (cotyledon, true leaves, hypocotyl, and petiole) dry weight of individual plants 216 h after sowing (HAS) (*Wd*) with nutrients and water.

Figure 4 illustrates the time course of the $Ap-c$ and $Ap-t$ of individual seedlings, both with nutrients and water from Hc to 216 HAS, each with distributions of horizontal PPFs (see Table 1 for treatments and codes). Note that some of the $Ap-c$ or $Ap-t$ at specific periods were not estimated because of the overlapping of the leaves. For some seedlings Hc could not be calculated, and the polygonal lines started 66.5 or 68 HAS with nutrients and water, respectively, in response to each \overline{Hc} .

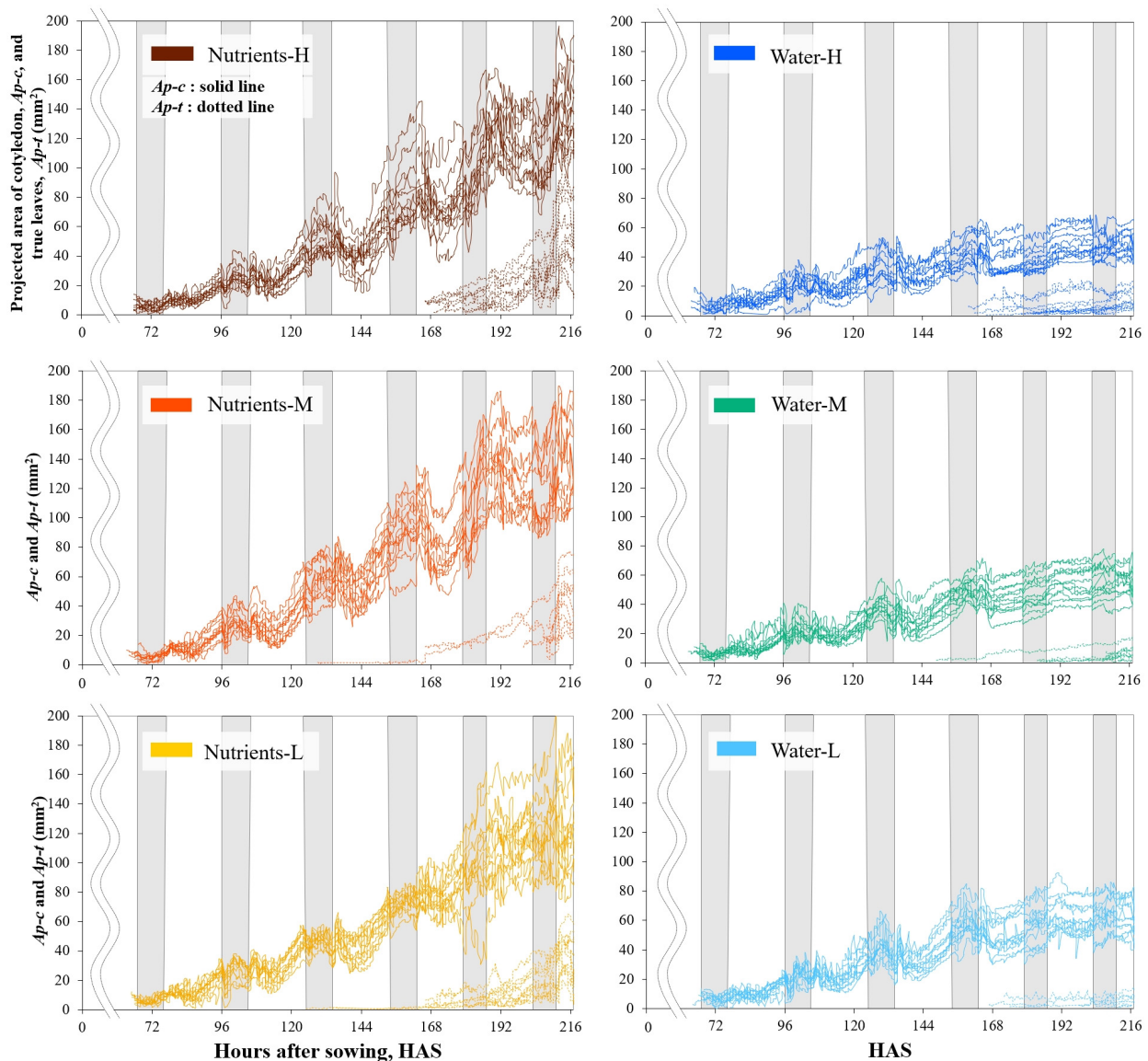


Figure 4. Time-course projected areas of the cotyledon ($Ap-c$) and true leaves ($Ap-t$) of individual seedlings with nutrients and water from hours to cotyledon unfolding from sowing (Hc) to 216 h after sowing (HAS), each with distributions of horizontal PPFs (see Table 1 for treatments and codes).

By estimating the projected areas of cotyledons and true leaves of individual seedlings separately, we demonstrated time-course changes of $Ap-c$ and $Ap-t$, respectively (Figure 4). The relative changes over time in projected areas within the single seedlings suggested the time series movement of cotyledons and true leaves, including changes in leaning or direction, in addition to the relative growth, depending on the viewing angle of the camera.

Although $Ap-c$ and $Ap-t$ with water remained reasonably constant over time, it caused a significant and continued increase in $Ap-c$ and $Ap-t$ with nutrients with more fluctuation over time. Indeed, a significant increase was found, especially in $Ap-t$ with nutrients. Furthermore, $Ap-c$ with nutrients continued to increase even after the initial development

of $Ap-t$ (Figure 4). It appeared that, particularly for $Ap-c$, a relative increase was caused mainly in the dark period, not the photoperiod (Figure 4). As clearly shown in Figure 4, this indicated a condition in which the relative growth in $Ap-c$ and $Ap-t$ was more extensive with a higher PPFD with nutrients. However, it was found that the time-course changes of individual seedlings with nutrients showed more considerable variations, compared to water (Figure 4).

Table 3 summarizes the average of Hc (\overline{Hc}), projected areas, including $\overline{Ap-c}$ both at cotyledon unfolding (Hc) and 216 HAS, and $\overline{Ap-t}$ and $\overline{Ap-ct}$ 216 HAS with nutrients and water, each with distributions of horizontal PPFDs (see Table 1 for treatments and codes). The slight difference in the initial $\overline{Ap-c}$ at cotyledon unfolding between the nutrients and water resulted in an approximately threefold difference in the $\overline{Ap-c}$ 216 HAS, along with $\overline{Ap-t}$, and thus, $\overline{Ap-ct}$ 216 HAS (Table 3). The $\overline{Ap-ct}$ with nutrients was more remarkable, in particular, caused by the growth of $\overline{Ap-t}$ (Table 3). As indicated in Table 3, $\overline{Ap-c}$, and especially $\overline{Ap-t}$ and $\overline{Ap-ct}$ 216 HAS, were larger with higher PPFD with nutrients.

Table 3. Average hours to cotyledon unfolding (\overline{Hc}), projected areas of cotyledon ($\overline{Ap-c}$) both at cotyledon unfolding and 216 h after sowing (HAS), true leaves ($\overline{Ap-t}$), and the sum of $Ap-c$ and $Ap-t$ ($\overline{Ap-ct}$), with nutrients and water, each with distributions of horizontal PPFDs (see Table 1 for treatments and codes).

Treatment Code	Hours to Cotyledon Unfolding (\overline{Hc}) ¹	Projected Cotyledon Area ($\overline{Ap-c}$) at Hc ²	$\overline{Ap-c}$ 216 HAS	Projected Area of True Leaves ($\overline{Ap-t}$) 216 HAS	Projected Area of Cotyledon and True Leaves ($\overline{Ap-ct}$) 216 HAS
	h	mm ²	mm ²	mm ²	mm ²
Nutrients-H	67	10	138	54	192
Nutrients-M	65	8	138	43	172
Nutrients-L	66	8	124	36	157
Water-H	69	9	49	11	58
Water-M	66	8	55	7	62
Water-L	69	11	64	6	67

¹ Percentage of identified Hc of seedlings that could be estimated from the time series images was 56% with nutrients and 67% with water. ² $\overline{Ap-c}$ at cotyledon unfolding.

Table 4 shows the average and coefficient of variation of the measured values 216 HAS, including areas of the cotyledon (Ac), true leaves (At) and the sum of individual Ac and At (Act), hypocotyl length (Lh), shoot fresh weight (Wf), shoot dry weight (Wd), and the ratio of Act to Wd (LAR) of individual seedlings with nutrients and water, each with distributions of horizontal PPFDs (see Table 1 for treatments and codes). The average Ac (\overline{Ac}), At (\overline{At}), and Act (\overline{Act}) values with nutrients were largest with Nutrients-H and the smallest with Nutrients-L. Furthermore, a greater coefficient of variation in Ac , At , and Act was shown with higher PPFD with nutrients, which was also demonstrated with Wf , Wd , and, to a lesser extent, with LAR (Table 4).

Figure 5a shows the Act at 216 HAS and $Ap-ct$ with nutrients and water. The value of $Ap-ct$ varied depending on the timing due to the movement of the plants. The $Ap-ct$ includes its values at 216 HAS and the maximum value over 216 h (MAX) (Figure 5a). The results showed that although the maximum $Ap-ct$ over 216 h was slightly closer to the Act , the overall Act was greater than $Ap-ct$, notably with the nutrients (Figure 5a). Figure 2b shows the RGB image of the largest $Ap-ct$ (with Nutrients-H) among 72 seedlings 216 HAS. In addition to the changes in the leaning of cotyledons and true leaves, slightly curled up cotyledon or true leaves decreased the value of $Ap-ct$ (Figure 2b).

Figure 5b illustrates the ratio between $Ap-ct$ and Act and Wd of individual seedlings at 216 HAS with nutrients and water. This implied that the ratio between $Ap-ct$ and Act 216 HAS did not have an impact on the Wd of individual seedlings, but only suggested a significant difference in Wd affected by the difference in nutrients and water (Figure 5b). The

average ratio between $Ap-ct$ and Act among individual seedlings with nutrients and water was 0.59 and 0.70, respectively, resulting in a greater average ratio of water to nutrients.

Table 4. Average and coefficient of variation of areas of the cotyledon (Ac), true leaves (At), and the sum of individual Ac and At (Act), hypocotyl length (Lh), shoot (cotyledon, true leaves, hypocotyl, and petiole) fresh weight (Wf), shoot dry weight (Wd), and the ratio of Act to Wd (LAR) of individual seedlings measured respectively 216 h after sowing (HAS) with nutrients and water, each with distributions of horizontal PPFs (see Table 1 for treatments and codes).

	Treatment Code	Area of Cotyledon (Ac)	Area of True Leaves (At)	Area of Cotyledon and True Leaves (Act)	Hypocotyl Length (Lh)	Shoot Fresh Weight (Wf)	Shoot Dry Weight (Wd)	The Ratio of Act to Wd (Act/Wd) (LAR)
		mm ²	mm ²	mm ²	mm	mg	mg	m ² g ⁻¹
Average	Nutrients-H	206	110	316	12	83.6	6.2	51
	Nutrients-M	205	102	307	13	84.0	6.0	52
	Nutrients-L	187	86	273	15	70.0	4.7	58
Coefficient of variation	Nutrients-H	0.131	0.258	0.157	0.139	0.206	0.208	0.096
	Nutrients-M	0.101	0.219	0.126	0.183	0.140	0.169	0.095
	Nutrients-L	0.101	0.123	0.090	0.137	0.058	0.095	0.081
Average	Water-H	71	14	84	10	24.5	3.3	26
	Water-M	72	15	88	10	25.2	2.9	30
	Water-L	82	13	96	12	26.9	2.7	36
Coefficient of variation	Water-H	0.155	0.315	0.138	0.147	0.167	0.195	0.222
	Water-M	0.260	0.675	0.210	0.148	0.164	0.205	0.156
	Water-L	0.159	0.385	0.187	0.112	0.209	0.208	0.150

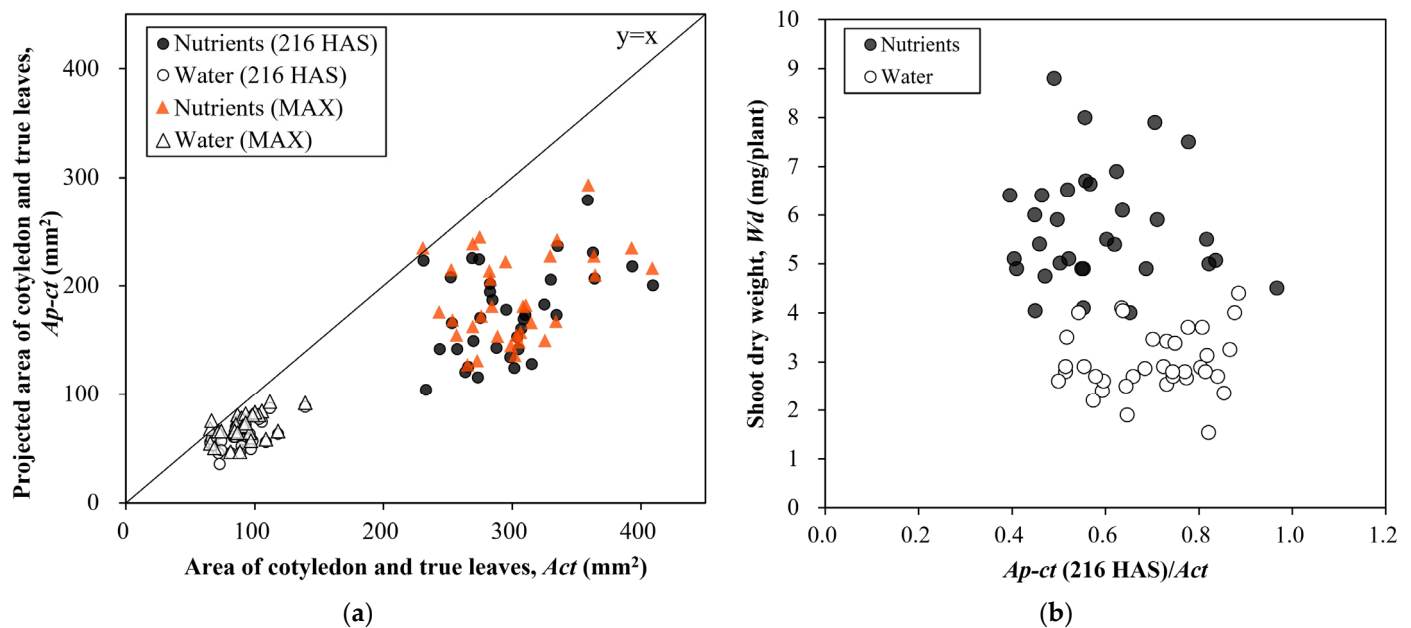


Figure 5. (a) The projected area of cotyledon and true leaves of the individual plants ($Ap-ct$) and area of cotyledon and true leaves of individual plants 216 h after sowing (HAS) (Act), with nutrients and water. The $Ap-ct$ includes its value at 216 HAS and the maximum value over 216 h. (b) The ratio between $Ap-ct$ and Act ($Ap-ct/Act$) together with shoot (cotyledon, true leaves, hypocotyl, and petiole) dry weight (Wd) all at 216 HAS with nutrients and water.

Figure 6 illustrates the integrated PPF from Hc to 216 HAS of each seedling and Wd with nutrients and water, each with distributions of horizontal PPFs (see Table 1 for treatments and codes). Note that for some seedlings Hc could not be identified; those Hc were assumed to be \overline{Hc} of 66.5 or 68 HAS with nutrients and water, respectively. This

resulted in a greater Wd with nutrients, particularly with Nutrients-H, compared with water, as demonstrated in Figure 6. Furthermore, variations in Wd were found, especially with nutrients in the larger PPFD (Figure 6, Table 4). In fact, the coefficient of determination was small, both with nutrients and water (Figure 6).

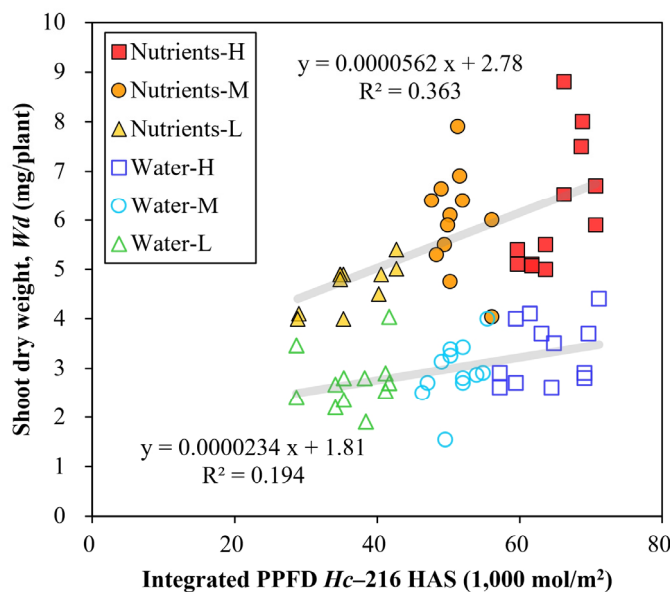


Figure 6. Integrated photosynthetic photon flux density (PPFD) from cotyledon unfolding (Hc) to 216 h after sowing (HAS) of each seedling and shoot (cotyledon, true leaves, hypocotyl, and petiole) dry weight of individual seedlings 216 HAS (Wd), with nutrients and water, each with distributions of horizontal PPFDs (see Table 1 for treatments and codes).

4. Discussion

The objective of this study was to analyze the variations in the growth of cotyledons and initial true leaves, as affected by the surrounding microenvironment of varied PPFDs at individual seedlings and nutrients or water, based on the time series RGB image data captured every 0.5 h, along with individual measurements at 216 HAS.

For this study, seedlings, one of the critical initial stages of plant growth, were used as part of the plant cohort research with the MSPS, developed by improving a GCB equipped with a phenotyping unit and air temperature and relative humidity sensors [5]. The MSPS was designed with the high priority of installing cameras and sensors with low cost and compactness, emphasizing the practicality and scalability in commercial plant production and selection of seedlings for grading and breeding in PFALs.

In this study, the Hc of individual seedlings was estimated using the time course of the RGB images of individual seedlings. As Hc and Wd with nutrients and water demonstrated in Figure 3, the Hc of even the majority of seedlings varied at a maximum of 7 h, from 63–70 h. Although most cotyledon unfolding occurred in the dark period in this study, the difference in Hc may affect the integrated PPFD at each seedling in the case of the photoperiod.

With this individual analysis, a particular outlier of three seedlings with water with Hc of 77.5, 78.5, and 79 h, was found. One, with an Hc of 77.5 h, reached the second largest Wd (4.0 mg/plant) among the seedlings with water despite the unfavorable start, which implies the possibility of a delay in germination for some reason. The results demonstrated that \bar{Hc} with nutrients was 1.8 h less than that with water (66.2 h with nutrients and 68 h with water). Moreover, variations in Hc with nutrients were smaller than those with water (Table 3). This indicates the possibility of promoting cotyledon unfolding by absorbing nutrients from radicles in addition to their heterotrophic nutrition from the albumen of their seeds, which reflects the fact that all the Hc with nutrients occurred in the dark period. Furthermore, it can be presumed that seed phenotyping before sowing, including

measuring the size, shape, or weight of seeds, enables the prediction of Hc or Ac at the cotyledon unfolding of the individual plant.

The results indicated that microenvironments, including varied PPFs and nutrients or water, affected the phenotype or growth of individual seedlings (Figures 4–6, Tables 3 and 4). The estimation of time series $Ap-c$ and $Ap-t$, every 0.5 h based on the RGB images, revealed the relative individual changes over time, affected by varied PPFs and the nutrients or water (Figure 4, Table 3). Figure 4 and Table 3 demonstrate that the initial $Ap-c$ of 72 individuals varied over time in response to the surrounding microenvironment. With water, $Ap-c$ remained comparatively constant even after the emergence of $Ap-t$, regardless of the PPF (Figure 4). In contrast, $Ap-c$ with nutrients resulted in a continued relative increase throughout the experiment, even during the expansion of $Ap-t$ (Figure 4). With the nutrients, $Ap-ct$ 216 HAS was the largest with Nutrients-H, and the smallest with Nutrients-L (Table 3).

Furthermore, Figure 4 demonstrates the time series movements of cotyledons and true leaves, including the changes in leaning or direction, in addition to the relative growth. As shown in Figure 4, each time-course $Ap-c$ fluctuated more with the nutrients than with water. Indeed, the value of $Ap-ct$ varies depending on the timing of the movement of plants. However, even with the maximum $Ap-ct$ over 216 h, the result showed that the measured value, Act , was greater than $Ap-ct$ 216 HAS, particularly with the nutrients (Figure 5a). Interestingly, the difference between $Ap-ct$ and Act was caused by slightly curled up cotyledons or true leaves, and the changes in those leanings (Figure 2b). When comparing $Ap-ct$ and Act at a specific moment, the ratio between $Ap-ct$ and Act 216 HAS did not impact Wd of individual seedlings, but only suggested a significant difference in Wd affected by the difference in the nutrients and water (Figure 5b).

As shown in Figure 6 and Table 4, Wd was two-fold greater with nutrients than with water, resulting in a larger Wd with Nutrients-H. Although Wd was the largest with Nutrients-H and the smallest with Nutrients-L, it showed variations in Wd , especially with nutrients in the larger PPF (Figure 6, Table 4). In this respect, the coefficient of determination was small, both with the nutrients and water, i.e., 0.363 and 0.194, respectively (Figure 6). Furthermore, Table 4 shows a greater coefficient of variation in Wd with higher PPF with nutrients (Nutrients-H 0.208, Nutrients-M 0.169, and Nutrients-L 0.095 for Wd), along with Wf , Ac , At , Act , and, to a lesser extent, LAR .

We acknowledge that this study has some limitations. First, a single RGB camera covered one tray to obtain the projected images; the viewing angle was not adjusted before estimating $Ap-c$ or $Ap-t$. The growth variations were identified together with the actual measurements at 216 HAS (Figures 4 and 6, Table 4). In future studies, the image capturing method can be improved in parallel with evaluating the light environment, which enables the estimation of time series leaf areas, leaf angles, and integrated photosynthetic photons received by individual leaves.

Second, there were limitations in estimating Hc based on RGB images. In practice, there were several obstacles in determining Hc , also in association with estimating $Ap-c$ and $Ap-t$; seed coats remained attached to the cotyledon for some seedlings. Similar to the case of overlapping leaves, these issues will be resolved in future studies by improving the phenotyping system and applying automated determination of Hc , $Ap-c$, $Ap-t$, and $Ap-ct$ by incorporating artificial intelligence (AI), along with analyzing the effects of additional microenvironment and management factors on the phenotype of individual plants.

In this study, by estimating Hc and time series $Ap-c$, $Ap-t$, and $Ap-ct$, in concurrence with the individual measurements of Ac , At , Act , Wd , and Wf , the variations in seedling growth were identified even under a similar microenvironment, including PPF at individual seedlings and nutrients or water. Furthermore, the results demonstrated larger growth variations in the seedlings with higher relative growth with nutrients and larger PPF. This may have been caused by the differences in seed lot with the same variety and genotypes, or by other microenvironmental effects, among other factors. In PFALs, where plant growth can be accelerated by environmental control, it is crucial to consider

the effects of the microenvironment and uniformity of plant phenotype or growth. Based on the plant cohort research, selection of seedlings for grading and breeding along with plant production in PFALs may enable uniformity of plant phenotype or growth and high productivity in commercial plant production, in view of simplified interactions of plant phenotypes with the microenvironment, management, and genotype for the life cycle of the plant.

5. Conclusions

In this study, experiments on the initial stage of seedlings, which strongly affect plant productivity, were conducted to analyze how the surrounding microenvironment of PPFs and nutrients affects the variations in the growth of individual seedlings as part of research into the entire plant life cycle. A modular plant phenotype measurement system for seedling production was developed, which was designed with the high priority of installing cameras and sensors with low cost and compactness, emphasizing the system's practicality and scalability in commercial plant production in PFALs.

Using time series RGB images, cotyledon unfolding time and the time series projected area of cotyledons and true leaves of individual seedlings were obtained. In agreement with the actual individual measurements, variations in seedling growth were identified even under similar microenvironments. Furthermore, the results demonstrated larger variations in seedlings with higher relative growth.

With a view to simplifying interactions of plant phenotypes with the microenvironment, management, and genotype for the life cycle of the individual plant, selection of seedlings for grading and breeding, along with plant production in PFALs, may enable uniformity of plant phenotype or growth and higher productivity in PFALs.

Author Contributions: Conceptualization, E.H., T.K. and T.M.; methodology, E.H., Y.A. and T.K.; validation, E.H. and Y.A.; formal analysis, E.H., Y.A. and M.J.; investigation, E.H. and Y.A.; data curation, Y.A.; writing—original draft preparation, E.H.; writing—review and editing, E.H., Y.A., T.K., T.M., A.N., S.T. and M.J.; visualization, E.H. and Y.A.; supervision, E.H. and M.J. All authors have read and agreed to the published version of the manuscript.

Funding: This research received no external funding.

Data Availability Statement: All data are available in the paper.

Acknowledgments: The authors express their deep appreciation to Yoshiko Komaba, Na Lu, Osamu Nunomura, and Shin Watanabe for their technical support for the experimental setup and experiments.

Conflicts of Interest: The authors declare no conflict of interest.

References

1. Goto, E. Plant production in a closed plant factory with artificial lighting. *Acta Hort.* **2012**, *956*, 37–49. [[CrossRef](#)]
2. Kozai, T. Resource use efficiency of closed plant production system with artificial light: Concept, estimation and application to plant factory. *Jpn. Acad. Ser. B Phys. Biol. Sci.* **2013**, *89*, 447–461. [[CrossRef](#)]
3. Leong, R.; Urano, D. Molecular Breeding for Plant Factory: Strategies and Technology. In *Smart Plant Factory: The Next Generation Indoor Vertical Farms*; Springer: Berlin, Germany, 2018; pp. 301–323. [[CrossRef](#)]
4. Kozai, T.; Amagai, Y.; Hayashi, E. Towards sustainable plant factories with artificial lighting (PFALs): From greenhouses to vertical farms. In *Achieving Sustainable Greenhouse Cultivation*; Marcelis, L., Heuvelink, E., Eds.; Burleigh Dodds Science Publishing: Cambridge, UK, 2019; pp. 177–204.
5. Hayashi, E.; Amagai, Y.; Maruo, T.; Kozai, T. Phenotypic Analysis of Germination Time of Individual Seeds Affected by Microenvironment and Management Factors for Cohort Research in Plant Factory. *Agronomy* **2020**, *10*, 1680. [[CrossRef](#)]
6. Kozai, T.; Hayashi, E.; Amagai, Y. Plant factories with artificial lighting (PFALs) toward sustainable plant production. *Acta Hort.* **2020**, *1273*, 251–260. [[CrossRef](#)]
7. Ohyama, K.; Yamaguchi, J.; Enjoji, A. Resource Utilization Efficiencies in a Closed System with Artificial Lighting during Continuous Lettuce Production. *Agronomy* **2020**, *10*, 723. [[CrossRef](#)]
8. Orsini, F.; Pennisi, G.; Zulfiqar, F.; Gianquinto, G. Sustainable use of resources in plant factories with artificial lighting (PFALs). *Eur. J. Hortic. Sci.* **2020**, *85*, 297–309. [[CrossRef](#)]
9. SharathKumar, M.; Heuvelink, E.; Marcelis, L.F. Vertical farming: Moving from genetic to environmental modification. *Trends Plant Sci.* **2020**, *25*, 724–727. [[CrossRef](#)]

10. van Delden, S.; SharathKumar, M.; Butturini, M.; Graamans, L.; Heuvelink, E.; Kacira, M.; Kaiser, E.; Klamer, R.; Klerkx, L.; Kootstra, G. Current status and future challenges in implementing and upscaling vertical farming systems. *Nat. Food* **2021**, *2*, 944–956. [[CrossRef](#)]
11. Kozai, T. Benefits, problems and challenges of plant factories with artificial lighting (PFALs): A short review. *Acta Hort.* **2018**, *1227*, 25–30. [[CrossRef](#)]
12. Kozai, T.; Uraisami, K.; Kai, T.; Hayashi, E. Indexes, definition, equation and comments on productivity of plant factory with artificial lighting. *Nogyo Oyobi Engei* **2019**, *94*, 661–672. (In Japanese)
13. Kozai, T.; Uraisami, K.; Kai, K.; Hayashi, E. Productivity: Definition and application. In *Plant Factory Basics, Applications and Advances*; Kozai, T., Niu, G., Masabni, J., Eds.; Elsevier: Amsterdam, The Netherlands, 2022; pp. 197–216. [[CrossRef](#)]
14. Kozai, T.; Lu, N.; Hasegawa, R.; Nunomura, O.; Nozaki, T.; Amagai, Y.; Hayashi, E. Plant Cohort Research and Its Application. In *Smart Plant Factory: The Next Generation Indoor Vertical Farms*; Kozai, T., Ed.; Springer: Berlin, Germany, 2018; pp. 413–431. [[CrossRef](#)]
15. Nagano, S.; Moriyuki, S.; Wakamori, K.; Mineno, H.; Fukuda, H. Leaf-movement-based growth prediction model using optical flow analysis and machine learning in plant factory. *Front. Plant Sci.* **2019**, *10*, 227. [[CrossRef](#)]
16. Akiyama, T.; Kozai, T. Light Environment in the Cultivation Space of Plant Factory with LEDs. In *LED Lighting for Urban Agriculture*; Kozai, T., Fujiwara, K., Runkle, E., Eds.; Springer Nature: Singapore, 2016; pp. 91–109. [[CrossRef](#)]
17. Kim, J.; Kang, W.H.; Son, J.E. Interpretation and evaluation of electrical lighting in plant factories with ray-tracing simulation and 3D plant modeling. *Agronomy* **2020**, *10*, 1545. [[CrossRef](#)]
18. Saito, K.; Ishigami, Y.; Goto, E. Evaluation of the Light Environment of a Plant Factory with Artificial Light by Using an Optical Simulation. *Agronomy* **2020**, *10*, 1663. [[CrossRef](#)]
19. Kumar, J.; Pratap, A.; Kumar, S. *Phenomics in Crop Plants: Trends, Options and Limitations*; Springer: New Delhi, India, 2015; p. 296.
20. Fiorani, F.; Schurr, U. Future scenarios for plant phenotyping. *Annu. Rev. Plant. Biol.* **2013**, *64*, 267–291. [[CrossRef](#)]
21. Golbach, F.; Kootstra, G.; Damjanovic, S.; Otten, G.; van de Zedde, R. Validation of plant part measurements using a 3D reconstruction method suitable for high-throughput seedling phenotyping. *Mach. Vis. Appl.* **2016**, *27*, 663–680. [[CrossRef](#)]
22. Guo, W. Automated characterization of plant growth and flowering dynamics using RGB images. In *Smart Plant Factory: The Next Generation Indoor Vertical Farms*; Springer: Berlin, Germany, 2018; pp. 385–393. [[CrossRef](#)]
23. Shibata, T.; Iwao, K.; Takano, T. Growth prediction of lettuce plants by image processing. *Acta Hort.* **1992**, *319*, 689–694. [[CrossRef](#)]
24. Giacomelli, G.A.; Ling, P.P.; Morden, R.E. An automated plant monitoring system using machine vision. *Acta Hort.* **1996**, *440*, 377–382. [[CrossRef](#)]
25. Itoh, H.; Yamamoto, H. A Modeling of Lettuce Growth by System Identification (Part 1). *J. Jpn. Soc. Agric. Mach.* **2005**, *67*, 71–80. (In Japanese)
26. Franchetti, B.; Ntouskos, V.; Giuliani, P.; Herman, T.; Barnes, L.; Pirri, F. Vision based modeling of plants phenotyping in vertical farming under artificial lighting. *Sensors* **2019**, *19*, 4378. [[CrossRef](#)] [[PubMed](#)]
27. Jayalath, T.C.; van Iersel, M.W. Canopy Size and Light Use Efficiency Explain Growth Differences between Lettuce and Mizuna in Vertical Farms. *Plants* **2021**, *10*, 704. [[CrossRef](#)]
28. Tian, Z.; Ma, W.; Yang, Q.; Duan, F. Application status and challenges of machine vision in plant factory—A review. *Inf. Processing Agric.* **2021**. [[CrossRef](#)]
29. Kitajima, K. Impact of cotyledon and leaf removal on seedling survival in three tree species with contrasting cotyledon functions1. *Biotropica* **2003**, *35*, 429–434. [[CrossRef](#)]
30. Hanley, M.E.; May, O.C. Cotyledon damage at the seedling stage affects growth and flowering potential in mature plants. *New Phytol.* **2006**, *169*, 243–250. [[CrossRef](#)] [[PubMed](#)]
31. Zhang, H.; Zhou, D.; Matthew, C.; Wang, P.; Zheng, W. Photosynthetic contribution of cotyledons to early seedling development in *Cynoglossum divaricatum* and *Amaranthus retroflexus*. *N. Z. J. Bot.* **2008**, *46*, 39–48. [[CrossRef](#)]
32. Zheng, W.; Wang, P.; Zhang, H.; Zhou, D. Photosynthetic Characteristics of the Cotyledon and First True Leaf of Castor (*Ricinus communis* L.). *Aust. J. Crop. Sci.* **2011**, *5*, 702–708. [[CrossRef](#)]
33. Kikuzawa, K. The basis for variation in leaf longevity of plants. *Vegetatio* **1995**, *121*, 89–100. [[CrossRef](#)]
34. Santos, H.P.; Buckeridge, M.S. The role of the storage carbon of cotyledons in the establishment of seedlings of *Hymenaea courbaril* under different light conditions. *Ann. Bot.* **2004**, *94*, 819–830. [[CrossRef](#)]
35. Walter, A.; Scharr, H.; Gilmer, F.; Zierer, R.; Nagel, K.A.; Ernst, M.; Wiese, A.; Virnich, O.; Christ, M.M.; Uhlig, B. Dynamics of seedling growth acclimation towards altered light conditions can be quantified via GROWSCREEN: A setup and procedure designed for rapid optical phenotyping of different plant species. *New Phytol.* **2007**, *174*, 447–455. [[CrossRef](#)] [[PubMed](#)]
36. Darwin, C.; Darwin, F. *The Power of Movement in Plants*; John Murray: London, UK, 1880.
37. Hoshi, T.; Takiguchi, T. Continuous Measurement of Movement in Spinach Leaves Using Video Cameras. *J. Agric. Meteorol.* **1995**, *51*, 123–130. (In Japanese) [[CrossRef](#)]
38. Hayashi, E.; Kozai, T. Phenotyping-and AI-Based Environmental Control and Breeding for PFAL. In *Smart Plant Factory: The Next Generation Indoor Vertical Farms*; Kozai, T., Ed.; Springer: Berlin, Germany, 2018; pp. 405–411.

39. Hasegawa, R. Data warehouse for plant phenotyping in plant factories. In Proceedings of the Japanese Society of Agricultural, Biological and Environmental Engineers and Scientists (JSABEES), Tokyo University of Ag. & Tech., Tokyo, Japan, 18–21 September 2018; pp. 224–225.
40. Schneider, C.A.; Rasband, W.S.; Eliceiri, K.W. NIH Image to ImageJ: 25 years of image analysis. *Nat. Methods* **2012**, *9*, 671–675. [[CrossRef](#)]
41. Maruo, T.; Ito, T.; Ishii, S. Studies on the feasible management of nutrient solution in hydroponically grown lettuce (*Lactuca sativa* L.). *Tech. Bull. Fac. Hortic. Chiba Univ.* **1992**, *46*, 235–240.